Coupling of two Dirac particles

Oleg L. Berman,[1,2] Roman Ya. Kezerashvili,[1,2] and Klaus Ziegler[3]

[1]*Physics Department, New York City College of Technology, The City University of New York, Brooklyn, New York 11201, USA*

[2]*The Graduate School and University Center, The City University of New York, New York, New York 10016, USA*

[3]*Institut für Physik, Universität Augsburg, D-86135 Augsburg, Germany*

(Received 17 February 2013; published 22 April 2013)

A study of the formation of excitons as a problem of two Dirac particles in a gapped graphene layer and in two gapped graphene layers separated by a dielectric is presented. In the low-energy limit the separation of the center-of-mass and relative motions is obtained. Analytical solutions for the wave function and energy dispersion for both cases when the electron and the hole interact via a Coulomb potential are found. It is shown that the energy spectrum and the effective exciton mass are functions of the energy gaps as well as of the interlayer separation in the case of two-layer gapped graphene.

DOI: 10.1103/PhysRevA.87.042513 PACS number(s): 31.15.ac, 03.65.Pm, 71.35.−y

I. INTRODUCTION

The coupling of two Dirac particles is of fundamental interest in both experimental and theoretical physics and is a subject of studies in different fields of physics. Usually the coupling of Dirac particles is considered using the Dirac equation or the field theoretic framework for the treatment of relativistic bound states in which the dynamics is governed by the Bethe-Salpeter equation. The canonical Foldy-Wouthuysen transformation [1] of the Dirac Hamiltonian allows one to obtain a two-component theory in the low-energy limit. In atomic physics the application of this approach as well as the Bethe-Salpeter formalism has led to the solution of the relativistic hydrogen problem, the bound states for a positronium [2] and a muonium [3]. For example, an effective Hamiltonian approach is considered for the perturbative calculation of bound state energies in positronium [2,4,5] that provides a sensitive test of the quantum electrodynamics. Let us also mention that Ref. [6] addresses that a Coulomb-like potential for the Dirac equation for which there is an exact SU(2) symmetry leads to an exact spin-orbit doublet degeneracy. References [7,8] provide examples of using in nuclear physics the Bethe-Salpeter formalism for the description of deuteron and the Foldy-Wouthuysen transformation for the effective electron-proton Hamiltonian retaining up through terms of order three of the inverse nucleon mass. In particle physics similar techniques for the coupling of two Dirac particles are used nowadays for describing quark-antiquark bound states and quarkonium, which is a fundamental problem in quantum chromodynamics (see, for example, Ref. [9]). To this type of system, where two Dirac particles are coupled, belongs also the exciton in graphene, a two-dimensional (2D) honeycomb lattice formed by carbon atoms [10,11]. At low energies an electron and a hole in graphene are described by a two-dimensional Dirac-like (Weyl-like) equation, in which the Fermi velocity plays the role of the speed of light [12–15].

The study of the excitonic system and its properties is necessary because of potential applications in electronics and photonics, including design of thresholdless lasers, optical computing, and quantum computing [16–23]. From the theoretical point of view, an exciton is a two-body system and to address the problem we have to solve a two-body problem in semiconductor heterostructures or graphene. Let us mention that the problem of the interaction between two particles is very important for an in-depth analysis of the many-body physics in an excitonic system. The analysis of the spectrum of collective excitations necessary to study such many-body phenomena in an excitonic system as Bose-Einstein condensation and superfluidity [24] requires the solution of a two-body problem for a single exciton. The temperature of the Kosterlitz-Thouless phase transition corresponding to superfluidity depends on the density of the superfluid component [25]. This density of the superfluid component is defined by the two-particle Green function of weakly interacting excitons. The problem of finding the two-particle Green function of the interacting excitons requires a one-particle Green function of the noninteracting excitons, which is defined by the wave function and energy dispersion of a single exciton [26]. The collective properties and superfluidity of excitons and polaritons in gapped graphene have been studied in Refs. [27,28]. Therefore, it is of fundamental and practical interest to focus on the solution of the two-body problem in semiconductor heterostructures and graphene. Finding the solution of the two-body problem in gapped graphene layers is the subject of this paper.

To describe the formation of an exciton in semiconductor heterostructures like quantum wells the standard quantum mechanical approach is used based on the Schrödinger equation. In this case the two-body problem with a scalar interparticle potential is completely understood and developed both in configuration or momentum 3D as well as 2D spaces [29–31]. The notions of absolute time and absolute space allow us to describe the two particles of masses $m_1$and m_2 with Euclidean position vectors $\mathbf{r}_1$ and $\mathbf{r}_2$ and momenta $\mathbf{p}_1$ and $\mathbf{p}_2$ in an inertial frame. It is well known [29] that, in covariant mechanics, the most straightforward solution of the classical problem with scalar interaction is obtained by a transformation from the individual particle coordinates $\mathbf{r}_1$ and $\mathbf{r}_2$ and $\mathbf{p}_1$ and $\mathbf{p}_2$ to the covariant center-of-mass and relative coordinates. Using canonical transformation,

$$\mathbf{R} = \frac{m_1\mathbf{r}_1 + m_2\mathbf{r}_2}{m}, \quad \mathbf{r} = \mathbf{r}_1 - \mathbf{r}_2, \\ \text{and } \mathbf{P} = \mathbf{p}_1 + \mathbf{p}_2, \quad \mathbf{p} = \mathbf{p}_1 - \mathbf{p}_2, \tag{1}$$

where $m = m_1 + m_2$ is the total mass of the system, we can separate the center-of-mass from the relative motion in configuration or momentum space. At these coordinates, the nontrivial motion of the system of two particles occurs entirely in the reduced problem of one-body motion and motion of the center-of-mass. The total Hamiltonian of the system can be presented as a sum of two parts. One part describes the motion of the center-of-mass while the other part describes two particles' relative motion: $H = \frac{\mathbf{P}^2}{2m} + H_r$ with $H_r = \frac{\mathbf{p}^2}{2\mu} + V(r)$, where $\mu = m_1 m_2/m$ is the two bodies' reduced mass. The Hamiltonian H_r governs the relative motion of two particles and, when the Schrödinger equation with this Hamiltonian has been solved, the wave function of the relative motion of two particles is obtained.

Today graphene has been attracting a great deal of experimental and theoretical attention because of unusual properties in its band structure [14,32–34]. Graphene is a 2D layer of carbon atoms, where the atoms form a honeycomb lattice [10,11]. In the low-energy limit the low-energy excitations in graphene are described not by the Schrödinger equation but instead, in graphene, electrons and holes behave as relativistic massless particles described by a Dirac-like equation for massless and chiral particles [12–15], which is known as the Weyl equation. Many of the unusual properties of graphene arise from the fact that its quasiparticles are described by Dirac spinors. Since electrons and holes in graphene are governed by the Weyl equation they have an intrinsic degree of freedom that resembles the spin degree of freedom in the original Weyl equation. This degree of freedom is called pseudospin in order to distinguish it from the spin and is described by the Pauli matrices. In connection with the pseudospin, there is a good quantum number—the chirality that is defined to be the projection of the two-momentum operator in the direction of the pseudospin. Clearly, the electrons will have positive chirality and the holes will have negative chirality. Also the Fermi speed $v_F \sim 10^6$ m/s, which is around 300 times slower than the speed of light, replaces the speed of light in the original Weyl equation. The positive-energy solutions of this 2D equation describe electrons, whereas the negative-energy solutions describe holes.

A 2D exciton, which is a bound state of an interacting electron and hole, in gapped graphene presents a two-body system and it is a fundamental and practical interest to focus on the solution of the two-body problem in graphene. Graphene consists of two equivalent carbon sublattices and quantum-mechanical hopping between the sublattices leads to the formation of two energy bands, and their intersection near the edges of the Brillouin zone yields the conical energy spectrum. As a result, quasiparticles in graphene exhibit a linear dispersion relation. The formation of excitons requires the existence of the energy gap in the electron and hole energy spectrum. The formation of excitons in gapped graphene was studied in Refs. [27,35–37]. The electronic ground state of intrinsic graphene and bilayer graphene in the absence of the energy gap using density functional theory within the local-density approximation and the Bethe-Salpeter equation was studied in Ref. [38]. According to Ref. [38], no pure bound exciton was identified in intrinsic graphene and bilayer graphene in the absence of the energy gap. Therefore, excitons in graphene can be formed due to an energy gap opening in the electron and hole spectra in the graphene layer. There are different mechanisms of electronic excitations in graphene. The energy gap in graphene can be induced and controlled by a magnetic field, by doping, by an electric field in biased graphene, and by hydrogenation [35,39–41].

By contrast, in quantum mechanics the description of the relativistic two-body problem is extremely more complicated and till now there has been no completely self-consistent theory for the separation of the center-of-mass and relative motions even for the two-body case. This is due to the following facts.

(i) The particles' locations and momenta are four-vectors.

(ii) The momenta are not independent but must satisfy mass-shell conditions.

(iii) The interparticle interaction potentials appear in the boosts as well as in the energy generator in the instant form of dynamics. As a result of a transformation to the center-of-mass system even a scalar action-at-a-distance interparticle interaction potential becomes dependent on a coordinate and momentum.

(iv) The structure of the Poincaré group implies that there is no definition of the relativistic 4-center-of-mass sharing all the properties of the nonrelativistic 3-center-of-mass [42].

The two-body problem in graphene when the electron and hole interact via a scalar action-at-a-distance interparticle potential and are described by Weyl's equation becomes even more complicated than in the simple relativistic case. First, this is related to the fact that the speed of light in the Weyl equation for an electron in graphene is replaced by the Fermi speed and the resultant equation becomes noncovariant and the canonical transformation implementing the separation of the center-of-mass from the relative variables within the relativistic approach is invalidated. Second, even though the interparticle interaction depends only on the coordinate of the relative motion, after the center-of-mass transformation it becomes dependent also on the momentum. Last, the center-of-mass cannot be separated from the relative motion even though the interaction depends only on the coordinate of the relative motion. This is caused by the chiral nature of Dirac electrons in graphene.

Our paper is organized in the following way. In Sec. II we present the Hamiltonian of the coupled two Dirac particles in the gapped graphene. In Sec. III we present the procedure of separation of the center-of-mass and relative motions for two particles in graphene. In Sec. IV we obtain the energy spectrum and the wave function of dipole excitons in two-layer graphene and find the effective exciton mass. The energy spectrum and the wave function of excitons formed in a gapped graphene layer and the corresponding effective exciton mass are given in Sec. V. Finally, the conclusions follow in Sec. VI.

II. EXCITON HAMILTONIAN

Let us consider two different parallel graphene layers with the interlayer separation D and assume that excitons in this system are formed by the electrons located in the one graphene layer and, correspondingly, the holes located in the other. In this system electrons and holes move in two separate layers with a honeycomb lattice structure. Since the motion of the electron is restricted in one graphene layer and the motion of the hole is restricted in the other graphene layer, we replace the

coordinate vectors of the electron and hole by their projections $\mathbf{r}_1$ and $\mathbf{r}_2$ on the plane of one of the graphene sheets. These new in-plane coordinates $\mathbf{r}_1$ and $\mathbf{r}_2$ are used everywhere below. Thus, we reduced the restricted 3D two-body problem to the 2D two-body problem on the graphene plane. Each honeycomb lattice is characterized by the coordinates $(\mathbf{r}_j,1)$ on sublattice A and the coordinates $(\mathbf{r}_j,2)$ on sublattice B with $j=1$ and 2 referring to the two sheets. Then the two-particle wave function, describing two particles in different sheets, reads $\Psi(\mathbf{r}_1,s_1;\mathbf{r}_2,s_2)$, where $\mathbf{r}_1$ and $\mathbf{r}_2$ represent the coordinates of the electron and the hole, repectively, and s_1 and s_2 are sublattice indices. This wave function can also be understood as a four-component spinor, where the spinor components refer to the four possible values of the sublattice indicies s_1 and s_2:

$$\Psi(\mathbf{r}_1,s_1;\mathbf{r}_2,s_2)=\begin{pmatrix}\phi_{aa}(\mathbf{r}_1,\mathbf{r}_2)\\ \phi_{ab}(\mathbf{r}_1,\mathbf{r}_2)\\ \phi_{ba}(\mathbf{r}_1,\mathbf{r}_2)\\ \phi_{bb}(\mathbf{r}_1,\mathbf{r}_2)\end{pmatrix}\equiv\begin{pmatrix}\Psi_a\\ \Psi_b\end{pmatrix},$$
$$\text{where } \Psi_a=\begin{pmatrix}\phi_{aa}\\ \phi_{ab}\end{pmatrix},\quad \Psi_b=\begin{pmatrix}\phi_{ba}\\ \phi_{bb}\end{pmatrix}. \tag{2}$$

The two components mean that one particle is on sublattice A(B) and the other particle is on sublattice A(B), correspondingly. In other words, the spinor components are from the same tight-binding wave function at different sites. Each graphene layer has an energy gap. Obviously the energy gaps in graphene layers are independent and in the general case we can introduce two nonequal gaps, δ_1 and δ_2, for the first and the second graphene layers, respectively.

The corresponding hopping matrix for two noninteracting particles, including the energy gaps δ_1 and δ_2 on the first and second layers, respectively, then reads

$$\mathcal{H}_0=\begin{pmatrix}-\delta_1+\delta_2 & d_2 & d_1 & 0\\ d_2^\dagger & -\delta_1-\delta_2 & 0 & d_1\\ d_1^\dagger & 0 & \delta_1+\delta_2 & d_2\\ 0 & d_1^\dagger & d_2^\dagger & \delta_1-\delta_2\end{pmatrix}. \tag{3}$$

In Eq. (3) $d_1=\hbar v_F(-i\partial_{x_1}-\partial_{y_1})$ and $d_2=\hbar v_F(-i\partial_{x_2}-\partial_{y_2})$ and the corresponding Hermitian conjugates are $d_1^\dagger=\hbar v_F(-i\partial_{x_1}+\partial_{y_1})$ and $d_2^\dagger=\hbar v_F(-i\partial_{x_2}+\partial_{y_2})$, where $\partial_x=\partial/\partial x$ and $\partial_y=\partial/\partial y$; x_1, y_1 and x_2, y_2 are the coordinates of vectors $\mathbf{r}_1$ and $\mathbf{r}_2$, respectively; and v_F is the Fermi velocity of electrons in graphene. This Hamiltonian allows us to write the eigenvalue equation for two noninteracting particles as

$$\mathcal{H}_0\Psi_0=\epsilon_0\Psi_0, \tag{4}$$

which leads to the following eigenenergies:

$$\begin{aligned}\epsilon_0(k_1,\delta_1;k_2,\delta_2)&=\pm\sqrt{\hbar^2v_F^2k_1^2+\hbar^2v_F^2k_2^2+\delta_1^2+\delta_2^2\pm2\sqrt{(\hbar^2v_F^2k_1^2+\delta_1^2)(\hbar^2v_F^2k_2^2+\delta_2^2)}}\\&=\pm\sqrt{\hbar^2v_F^2k_1^2+\delta_1^2}\pm\sqrt{\hbar^2v_F^2k_2^2+\delta_2^2}.\end{aligned} \tag{5}$$

where k_1 and k_2 are the wave vector of each particle, correspondingly. Equation (5) gives the energy spectrum for two noninteracting particles in the presence of the nonequal gap energies δ_1 and δ_2. When there are no gaps, $\delta_1=0$ and $\delta_2=0$, as it follows from Eq. (5), the energy dispersion is $\pm\hbar v_Fk_1\pm\hbar v_Fk_2$.

Let's consider the electron and the hole located in two graphene sheets with the interlayer separation D, and interacting via the Coulomb potential $V(r)$, where r is the projection of the distance between an electron and a hole on the plane parallel to the graphene layers. Now the problem for the two interacting particles located in different graphene layers with the broken sublattice symmetry in each layer can be described by the Hamiltonian

$$\mathcal{H}=\begin{pmatrix}-\delta_1+\delta_2+V(r) & d_2 & d_1 & 0\\ d_2^\dagger & -\delta_1-\delta_2+V(r) & 0 & d_1\\ d_1^\dagger & 0 & \delta_1+\delta_2+V(r) & d_2\\ 0 & d_1^\dagger & d_2^\dagger & \delta_1-\delta_2+V(r)\end{pmatrix}, \tag{6}$$

and the eigenvalue problem for Hamiltonian (6) is

$$\mathcal{H}\Psi=\epsilon\Psi, \tag{7}$$

where Ψ are four-component eigenfunctions as given in Eq. (2).

Hamiltonian (6) describes two interacting particles located in two graphene layers and satisfies the following conditions.

(i) When both gaps vanish, $\delta_1=0$ and $\delta_2=0$, and the two-body potential $V(r)=0$, the Hamiltonian describes two noninteracting Dirac particles. It is important to mention that eigenenergies are symmetrical with respect to the replacement of particles 1 and 2.

(ii) When the interaction between particles vanishes, $V(r)=0$, the Hamiltonian describes two independent particles, each located in the separate graphene layers, having two independent gaps energies related to the broken sublattice symmetry in each graphene sheet.

(iii) When the gaps in each graphene layer vanish, $\delta_1=0$ and $\delta_2=0$, the Hamiltonian describes two interacting particles in one graphene layer interacting via the Coulomb potential $V(r)$ and is identical to the Hamiltonian (2) in Ref. [36] representing the two-body problem in one graphene layer if the band gap is absent.

(iv) When the gaps $\delta_1=\delta_2\equiv\delta$, the Hamiltonian describes two interacting particles in one graphene layer interacting via

the Coulomb potential $V(r) = -e^2/4\pi\varepsilon_0\varepsilon r$, where e is the charge of the electron and ε is the dielectric constant of the graphene layer.

(v) When an electron and a hole are located in two different graphene sheets with the interlayer separation D, they interact via the potential $V(r) = -e^2/4\pi\varepsilon_0\varepsilon_d\sqrt{r^2+D^2}$, where ε_d is the dielectric constant of the dielectric between the two graphene layers. Let us mention that for $\delta_1 = \delta_2 = 0$ and $D = 0$ Hamiltonian (6) is also identical to Hamiltonian (2) in Ref. [36].

III. SEPARATION OF THE CENTER-OF-MASS AND RELATIVE MOTIONS

In Hamiltonian (6) the center-of-mass cannot be separated from the relative motion even though the interaction $V = V(r)$ depends only on the coordinate of the relative motion. This is caused by the chiral nature of Dirac electrons in graphene. A similar conclusion was made for the two-particle problem in graphene in Ref. [36].

Since the electron-hole Coulomb interaction depends only on the relative coordinate, we introduce the new "center-of-mass" coordinates in the plane of a graphene sheet:

$$\mathbf{R} = \alpha\mathbf{r}_1 + \beta\mathbf{r}_2, \quad \mathbf{r} = \mathbf{r}_1 - \mathbf{r}_2. \tag{8}$$

Here the coefficients α and β are to be determined later. Apparently we can use the analogy of the two-particle problem for Dirac particles in gapped two-layer graphene with the center-of-mass coordinates for the case of the Schrödinger equation. The coefficients α and β are found below from the condition of the separation of the coordinates of the center-of-mass and relative motion in the Hamiltonian in the one-dimensional scalar equation determining the corresponding component of the wave function.

To find the solution of Eq. (7) we make the Ansätze

$$\Psi_j(\mathbf{R},\mathbf{r}) = e^{i\mathbf{K}\cdot\mathbf{R}}\psi_j(\mathbf{r}). \tag{9}$$

Let us introduce the following notations:

$$\mathcal{K}_+ = \mathcal{K}e^{i\Theta} = \mathcal{K}_x + i\mathcal{K}_y, \quad \mathcal{K}_- = \mathcal{K}e^{-i\Theta} = \mathcal{K}_x - i\mathcal{K}_y,$$
$$\Theta = \tan^{-1}\left(\frac{\mathcal{K}_y}{\mathcal{K}_x}\right), \tag{10}$$

and rewrite Hamiltonian (6) in terms of the representation of the coordinates $\mathbf{R}$ and $\mathbf{r}$ in the form of a 2×2 matrix as

$$\mathcal{H} = \begin{pmatrix} \mathcal{O}_2 + V(r)\sigma_0 - \delta_1\sigma_0 + \delta_2\sigma_3 & \mathcal{O}_1 \\ \mathcal{O}_1^\dagger & \mathcal{O}_2 + V(r)\sigma_0 - \delta_1\sigma_0 + \delta_2\sigma_3 \end{pmatrix}, \tag{11}$$

where $\mathcal{O}_1$ and $\mathcal{O}_2$ are given by

$$\mathcal{O}_1 = \hbar v_F(\alpha\mathcal{K}_- - i\partial_x - \partial_y)\sigma_0, \tag{12}$$

$$\mathcal{O}_2 = \hbar v_F \begin{pmatrix} 0 & \beta\mathcal{K}_- + i\partial_x + \partial_y \\ \beta\mathcal{K}_+ + i\partial_x - \partial_y & 0 \end{pmatrix}, \tag{13}$$

where x and y are the components of vector $\mathbf{r}$, σ_j are the Pauli matrices, and σ_0 is the 2×2 unit matrix. Analysis of the operators (12) and (13) shows that the coordinates of the center-of-mass and relative motion can be separated in a certain approximation.

For Hamiltonian (11) the eigenvalue problem $\mathcal{H}\Psi = \epsilon\Psi$ results in the following equations:

$$\begin{aligned} &[\mathcal{O}_2 + V(r)\sigma_0 - \delta_1\sigma_0 + \delta_2\sigma_3]\,\Psi_a + \mathcal{O}_1\Psi_b = \epsilon\sigma_0\Psi_a, \\ &\mathcal{O}_1^\dagger\Psi_a + [\mathcal{O}_2 + V(r)\sigma_0 - \delta_1\sigma_0 + \delta_2\sigma_3]\,\Psi_b = \epsilon\sigma_0\Psi_b. \end{aligned} \tag{14}$$

From Eq. (14) we have

$$\Psi_b = [\epsilon\sigma_0 - \mathcal{O}_2 - V(r)\sigma_0 + \delta_1\sigma_0 - \delta_2\sigma_3]^{-1}\,\mathcal{O}_1^\dagger\Psi_a. \tag{15}$$

Assuming the interaction potential and both the relative and center-of-mass kinetic energies are small compared to the gaps δ_1 and δ_2, we use the following approximation:

$$[\epsilon\sigma_0 - \mathcal{O}_2 - V(r)\sigma_0 + \delta_1\sigma_0 - \delta_2\sigma_3]^{-1} \simeq \frac{1}{\epsilon\sigma_0 + \delta_1\sigma_0 - \delta_2\sigma_3}. \tag{16}$$

Using the fact that the operator $\mathcal{O}_1^\dagger\mathcal{O}_1$ is purely Hermitian, applying Eq. (14) and

$$\mathcal{O}_1^\dagger\mathcal{O}_1 = \hbar^2 v_F^2\left[\alpha^2\mathcal{K}^2 - \nabla_{\mathbf{r}}^2 - 2i\alpha(\mathcal{K}_x\partial_y + \mathcal{K}_y\partial_x)\right]\sigma_0, \tag{17}$$

we obtain

$$[\mathcal{O}_2 + V(r)\sigma_0 - \delta_1\sigma_0 + \delta_2\sigma_3]\,\Psi_a + \hbar^2 v_F^2\frac{\left[\alpha^2\mathcal{K}^2 - \nabla_{\mathbf{r}}^2 - 2i\alpha(\mathcal{K}_x\partial_x + \mathcal{K}_y\partial_y)\right]}{\epsilon\sigma_0 + \delta_1\sigma_0 - \delta_2\sigma_3}\Psi_a = \epsilon\sigma_0\Psi_a. \tag{18}$$

Now using Eq. (2) we rewrite Eq. (18) for the individual spinor components in the following form:

$$\left[-\delta_1 + \delta_2 + V(r) + \hbar^2 v_F^2\frac{\alpha^2\mathcal{K}^2 - \nabla_{\mathbf{r}}^2 - 2i\hbar v_F\alpha(\mathcal{K}_x\partial_x + \mathcal{K}_y\partial_y)}{\epsilon - \delta_1 - \delta_2}\right]\phi_{aa} + \hbar v_F(\beta\mathcal{K}_- + i\partial_x + \partial_y)\phi_{ab} = \epsilon\phi_{aa}, \tag{19}$$

$$\hbar v_F(\beta\mathcal{K}_+ + i\partial_x - \partial_y)\phi_{aa} + \left[-\delta_1 - \delta_2 + V(r) + \hbar^2 v_F^2 \frac{\alpha^2\mathcal{K}^2 - \nabla_{\mathbf{r}}^2 - 2i\alpha(\mathcal{K}_x\partial_x + \mathcal{K}_y\partial_y)}{\epsilon - \delta_1 + \delta_2}\right]\phi_{ab} = \epsilon\phi_{ab}. \tag{20}$$

We solve Eq. (20) with respect to ϕ_{ab}:

$$\phi_{ab} = \left[\epsilon + \delta_1 + \delta_2 - V(r) - \hbar^2 v_F^2 \frac{\alpha^2\mathcal{K}^2 - \nabla_{\mathbf{r}}^2 - 2i\alpha(\mathcal{K}_x\partial_x + \mathcal{K}_y\partial_y)}{\epsilon - \delta_1 + \delta_2}\right]^{-1} (\beta\mathcal{K}_+ + i\partial_x - \partial_y)\hbar v_F\phi_{aa}. \tag{21}$$

Substituting ϕ_{ab} from Eq. (21) into Eq. (19), we obtain

$$\left[-\delta_1 + \delta_2 + V(r) + \hbar^2 v_F^2 \frac{\alpha^2\mathcal{K}^2 - \nabla_{\mathbf{r}}^2 - 2i\alpha(\mathcal{K}_x\partial_x + \mathcal{K}_y\partial_y)}{\epsilon - \delta_1 - \delta_2}\right]\phi_{aa} + \hbar^2 v_F^2(\beta\mathcal{K}_- + i\partial_x + \partial_y)$$
$$\times \left[\epsilon + \delta_1 + \delta_2 - V(r) - \hbar^2 v_F^2 \frac{\alpha^2\mathcal{K}^2 - \nabla_{\mathbf{r}}^2 - 2i\alpha(\mathcal{K}_x\partial_x + \mathcal{K}_y\partial_y)}{\epsilon - \delta_1 + \delta_2}\right]^{-1} (\beta\mathcal{K}_+ + i\partial_x - \partial_y)\varphi_{aa} = \epsilon\phi_{aa}. \tag{22}$$

Assuming again that the interaction potential and both the relative and center-of-mass kinetic energies are small compared to the gaps δ_1 and δ_2 we apply to Eq. (22) the following approximation:

$$\left[\epsilon + \delta_1 + \delta_2 - V(r) - \hbar^2 v_F^2 \frac{\alpha^2\mathcal{K}^2 - \nabla_{\mathbf{r}}^2 - 2i\alpha(\mathcal{K}_x\partial_x + \mathcal{K}_y\partial_y)}{\epsilon - \delta_1 + \delta_2}\right]^{-1} = \frac{1}{\epsilon + \delta_1 + \delta_2}. \tag{23}$$

Applying the approximation given by Eq. (23) to Eq. (22), we get from Eq. (22) the eigenvalue equation for the spinor component ϕ_{aa} in the following form:

$$\left[-\delta_1 + \delta_2 + V(r) + \hbar^2 v_F^2 \frac{\alpha^2\mathcal{K}^2 - \nabla_{\mathbf{r}}^2 - 2i\alpha(\mathcal{K}_x\partial_x + \mathcal{K}_y\partial_y)}{\epsilon - \delta_1 - \delta_2} + \hbar^2 v_F^2 \frac{\beta^2\mathcal{K}^2 - \nabla_{\mathbf{r}}^2 + 2i\beta(\mathcal{K}_x\partial_x + \mathcal{K}_y\partial_y)}{\epsilon + \delta_1 + \delta_2}\right]\phi_{aa} = \epsilon\phi_{aa}. \tag{24}$$

Choosing the values for the coefficients α and β to separate the coordinates of the center-of-mass (the wave vector $\mathcal{K}$) and relative motion $\mathbf{r}$ in Eq. (24), we have

$$\alpha = \frac{\epsilon - \delta_1 - \delta_2}{2\epsilon}, \quad \beta = \frac{\epsilon + \delta_1 + \delta_2}{2\epsilon}. \tag{25}$$

After substitution of Eq. (25) into Eq. (24) we can obtain the component ϕ_{aa} of the spinor (2) as a solution of one-dimensional second order differential equation:

$$\left\{\frac{(\hbar v_F\mathcal{K})^2}{2\epsilon} + V(r) - \frac{\epsilon(\hbar v_F)^2\nabla_{\mathbf{r}}^2}{2[\epsilon^2 - (\delta_1 + \delta_2)^2]}\right\}\phi_{aa}$$
$$= [\epsilon + \delta_1 - \delta_2]\phi_{aa}. \tag{26}$$

The other components of Eq. (2) can be found as

$$\Psi_b = -[\epsilon\sigma_0 - iD_2 - \delta_1\sigma_0 - \delta_2\sigma_3 - V(r)\sigma_0]^{-1} iD_1^\dagger\Psi_a, \tag{27}$$

with Pauli matrices σ_j and the 2×2 unit matrix σ_0. In Eq. (27), we have

$$D_1 = (\partial_{x_1} - i\partial_{y_1})\sigma_0, \quad D_2 = \partial_{x_2}\sigma_1 + \partial_{y_2}\sigma_2. \tag{28}$$

IV. TWO-BODY PROBLEM IN TWO GAPPED GRAPHENE LAYERS

Let us consider an electron and a hole located in two different parallel graphene layers and interacting via the potential $V(r) = -e^2/4\pi\varepsilon_0\varepsilon_d\sqrt{r^2 + D^2}$. Substituting this potential into Eq. (26) we obtain the second-order differential equation for the component ϕ_{aa}. This equation cannot be solved analytically. However, assuming $r \ll D$ we can approximate $V(r)$ by the first two terms of the Taylor series, and substituting $V(r) = -V_0 + \gamma r^2$, where $V_0 = e^2/4\pi\varepsilon_0\varepsilon_d D$ and $\gamma = e^2/8\pi\varepsilon_0\varepsilon_d D^3$ for the interaction potential into Eq. (26), we obtain

$$\left[-\frac{2\epsilon(\hbar v_F)^2\nabla_{\mathbf{r}}^2}{\epsilon^2 - (\delta_1 + \delta_2)^2} + \gamma r^2\right]\phi_{aa}$$
$$= \left[\epsilon + \delta_1 - \delta_2 + V_0 - \frac{(\hbar v_F\mathcal{K})^2}{2\epsilon}\right]\phi_{aa}. \tag{29}$$

The last equation can be rewritten in the form of the 2D isotropic harmonic oscillator:

$$\left[-\mathcal{F}_1(\epsilon)\nabla_{\mathbf{r}}^2 + \gamma r^2\right]\phi_{aa} = \mathcal{F}_0(\epsilon)\phi_{aa}, \tag{30}$$

where

$$\mathcal{F}_1 = \frac{2\epsilon(\hbar v_F)^2}{\epsilon^2 - (\delta_1 + \delta_2)^2}, \quad \mathcal{F}_0 = \epsilon + \delta_1 - \delta_2 + V_0 - \frac{(\hbar v_F\mathcal{K})^2}{2\epsilon}. \tag{31}$$

The eigenfunction and eigenenergy for the 2D isotropic parabolic well were first determined by Fock in 1928 [43], later in Ref. [44], and were studied in detail in Ref. [45]. The single-particle eigenfunction for the 2D oscillator was widely used for the description of quantum dots [46]. The solution of Eq. (30) is well known (see, for example, Ref. [47]) and is given by

$$\frac{\mathcal{F}_0(\epsilon)}{\mathcal{F}_1(\epsilon)} = 2N\sqrt{\frac{\gamma}{\mathcal{F}_1(\epsilon)}},$$

where $N = 2\tilde{N} + |L| + 1$, and $\tilde{N} = \min(\tilde{n},\tilde{n}')$, $L = \tilde{n} - \tilde{n}'$, and $\tilde{n}$, $\tilde{n}' = 0,1,2,3,\ldots$ are the quantum numbers of the 2D harmonic oscillator. The corresponding 2D wave function in

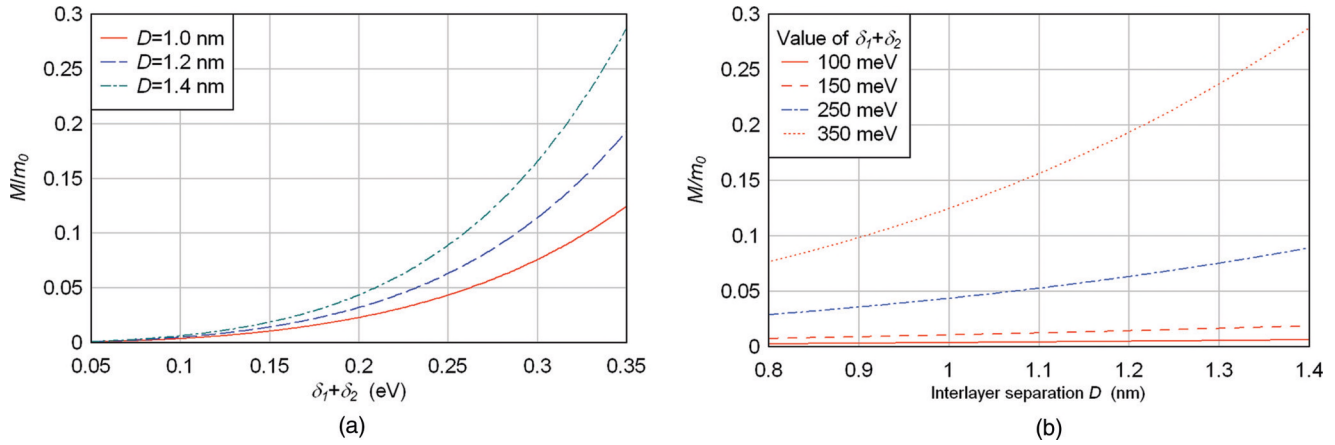

FIG. 1. (Color online) Excitons in two graphene layers separated by the dielectric GaAs. The effective exciton mass M in units of free electron mass m_0 (a) as a function of the total energy gap for the different graphene interlayer separations and (b) as the function of an interlayer separation for different values of the total energy gap.

terms of associated Laguerre polynomials can be written as

$$\phi_{aa_{\tilde{N}L}}(r) = \frac{\tilde{N}!}{a^{|L|+1}\sqrt{\tilde{n}!\tilde{n}'!}}\mathrm{sgn}(L)^L r^{|L|-1/2} e^{-r^2/(4a^2)} \times L_{\tilde{N}}^{|L|}[r^2/(2a^2)]\frac{e^{-iL\phi}}{(2\pi)^{1/2}}, \quad (32)$$

where ϕ is the polar angle, $L_k^p(x)$ are the associated Laguerre polynomials, and $a = [\sqrt{F_1(\epsilon)}/(2\sqrt{\gamma})]^{1/2}$.

After some straightforward but lengthy calculations and the expansion up to second order in $\mathcal{K}$ we obtain the following expression for the energy in quadratic order with respect to $\mathcal{K}$:

$$\epsilon = -V_0 + \sqrt{\mu^2 + \frac{C_1}{\mu}} + \frac{1}{2\mu^4}\frac{C_1}{\sqrt{1+\frac{C_1}{\mu^3}}}(\hbar v_F \mathcal{K})^2, \quad (33)$$

where $\mu = \delta_1 + \delta_2$ and $C_1 = 2\gamma N^2(\hbar v_F)^2$. Thus, from Eq. (33) we can conclude that the effective exciton mass M is given as a function of total energy gap $\delta_1 + \delta_2$ as

$$M = \frac{\mu^4}{v_F^2 C_1}\sqrt{1+\frac{C_1}{\mu^3}}. \quad (34)$$

The dependence of the effective exciton mass M defined by Eq. (34) on the total energy gap $\delta_1 + \delta_2$ and the interlayer separation D for two graphene layers separated by the dielectric GaAs is shown in Fig. 1. First, according to Fig. 1, the effective exciton mass M increases when the total energy gap $\delta_1 + \delta_2$ and the interlayer separation D increase. Second, the mass increases much faster for the bigger value of the interlayer separation and the bigger value of the energy gap. Note that the dependence of the effective exciton mass M on the interlayer separation D is caused by the quasirelativistic Dirac Hamiltonian of the gapped electrons and holes in graphene layers. However, for the excitons in coupled quantum wells (CQW) the effective exciton mass does not depend on the interlayer separation, because the electrons and holes in CQW are described by a Schrödinger Hamiltonian [48], while excitons in two graphene layers are described by the Dirac-like Hamiltonian (6).

In Fig. 2 is shown the energy dispersion of excitons for different values of the total energy gap and interlayer separation and for the different dielectrics between the graphene layers. Results are presented for the parabolic approximation for the energy dispersion assuming the low-energy limit. When $\mathcal{K} \sim 0.08\ \mathrm{nm}^{-1}$ the parabolic approximation (33) gives about 2% difference with respect to the exact numerical solution and this percentage decreases when $\mathcal{K}$ decreases. The analysis of the results presented in Fig. 2(a) shows that the energy dispersion decreases when the total energy gap increases. The same behavior can be observed for the dependence of the energy dispersion on interlayer separation: for given $\mathcal{K}$ when interlayer separation increases the energy dispersion decreases [Fig. 2(b)]. In Fig. 2(c) is given the energy dispersion of excitons for the different dielectric placed between two graphene layers. As can be seen, there is a small increase for the energy dispersion: for a smaller value of the dielectric constant the energy dispersion of excitons becomes bigger.

V. TWO-BODY PROBLEM IN A GAPPED GRAPHENE LAYER

Now we consider an electron and a hole located in a single gapped graphene layer with the energy gap parameter δ and an exciton formed by the electron and the hole located in this graphene layer. Putting the gaps $\delta_1 = \delta_2 \equiv \delta$ in Eq. (6), we obtain the Hamiltonian that describes two interacting particles in one graphene layer interacting via the Coulomb potential $V(r) = -\frac{e^2}{4\pi\varepsilon_0\varepsilon r}$. Using this potential we rewrite Eq. (26) in the form

$$\left[-\frac{2\epsilon(\hbar v_F)^2\nabla_{\mathbf{r}}^2}{\epsilon^2 - 4\delta^2} - \frac{e^2}{4\pi\varepsilon_0\varepsilon r}\right]\phi_{aa} = \left[\epsilon - \frac{(\hbar v_F \mathcal{K})^2}{2\epsilon}\right]\phi_{aa}. \quad (35)$$

Equation (35) can be rewritten in the form of the two-dimensional hydrogen atom:

$$\left(-\mathcal{F}_1(\epsilon)\nabla_r^2 - \frac{e^2}{4\pi\varepsilon_0\varepsilon r}\right)\phi_{aa} = \mathcal{F}_0(\epsilon)\phi_{aa}, \quad (36)$$

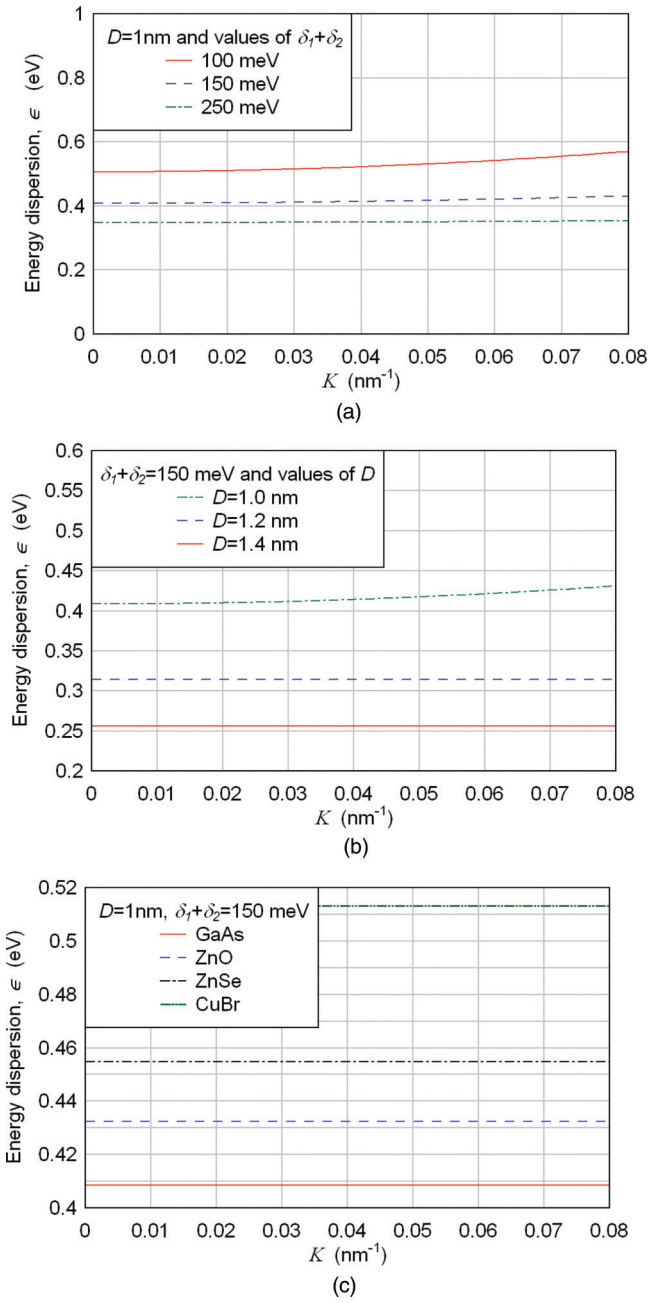

FIG. 2. (Color online) Excitons in two graphene layers separated by the dielectric. The energy dispersion of excitons in the ground state (a) for the fixed total energy gap and the different graphene interlayer separations, (b) for the fixed interlayer separation for different values of the total energy gap, and (c) for the fixed total energy gap, graphene interlayer separations, and the different dielectrics between graphene layers.

where

$$\mathcal{F}_1 = \frac{2\epsilon(\hbar v_F)^2}{\epsilon^2 - 4\delta^2}, \quad \mathcal{F}_0 = \epsilon - \frac{(\hbar v_F \mathcal{K})^2}{2\epsilon}. \tag{37}$$

The solution of the 2D hydrogen atom equation (36) is well known [49–51] and is given by

$$\mathcal{F}_0(\epsilon) = -\frac{e^4}{4\mathcal{F}_1(\epsilon)\varepsilon^2 (n-1/2)^2}, \tag{38}$$

where $n = 1,2,3,\ldots$ are the quantum numbers, and the wave function in terms of associated Laguerre polynomials is given by

$$\phi_{aa_{nl}}(\mathbf{r}) = \tilde{\beta}\left[\frac{(n-1-|l|)!}{[(|l|+n-1)!]^3(2n-1)}\right]^{1/2} \times e^{-\tilde{\beta}r/2}(\tilde{\beta}r)^{|l|} L^{2|l|}_{n+|l|-1}(\tilde{\beta}r)\frac{e^{il\varphi}}{(2\pi)^{1/2}}, \tag{39}$$

where $\tilde{\beta} = e^2/[(n-1/2)\varepsilon\mathcal{F}_1(\epsilon)]$, φ is the polar angle, $L^p_k(x)$ are the associated Laguerre polynomials, and the quantum numbers l can take the values $l = 0, \pm 1, \pm 2, \ldots, \pm(n-1)$.

After simplification Eq. (38) can be rewritten in the form of the following quadratic equation:

$$(C + 8\gamma)\epsilon^2 - 4\gamma k^2 - 4C\delta^2 = 0, \tag{40}$$

where $\gamma = (\hbar v_F)^2$, $k = \hbar v_F \mathcal{K}$, and $C = e^4/[4\pi\varepsilon_0\varepsilon(n-1/2)]^2$.

The solutions of Eq. (40) are given by

$$\epsilon = 2\left(\frac{\gamma(\hbar v_F\mathcal{K})^2 + C\delta^2}{C + 8\gamma}\right)^{1/2}. \tag{41}$$

Equation (41) gives the energy dispersion $\epsilon(\mathcal{K})$ of the electron and the hole that are bound via the Coulomb potential in a single graphene layer. Since our interest is small kinetic energy, therefore for small $\mathcal{K}$ we expand Eq. (41) with respect to $\mathcal{K}^2$ and approximate $\epsilon(\mathcal{K})$ by the first two terms of the Taylor series:

$$\epsilon = E_b + \frac{(\hbar\mathcal{K})^2}{2\mathcal{M}}, \tag{42}$$

where E_b is the exciton binding energy given by

$$E_b = 2\delta\left(\frac{C}{C + 2\gamma}\right)^{1/2} \tag{43}$$

and $\mathcal{M}$ is the effective mass of the exciton given by

$$\mathcal{M} = \frac{\delta}{2\gamma v_F^2}\sqrt{(C + 8\gamma)C}. \tag{44}$$

We note the exciton effective mass $\mathcal{M}$ increases when the gap δ increases as is shown in Fig. 3(a). The result of the calculation of the exciton energy dispersion in a graphene layer for different gap energy δ in the low-energy parabolic approximation is given in Fig. 3(b). When $\mathcal{K} \sim 0.08$ nm^{-1} the parabolic approximation (42) gives less than 0.5% difference with respect to the exact solution (41) and this value decreases when $\mathcal{K}$ decreases. According to Fig. 3(b), the energy dispersion of the exciton increases with the increase of the gap energy δ. However, for two graphene layers separated by a dielectric the energy dispersion decreases when the total energy gap increases. Also the comparison of the exciton energy distribution in a graphene layer and in two graphene layers separated by a dielectric shows that the exciton energy in a single graphene layer is always bigger than that in two graphene layers separated by a dielectric.

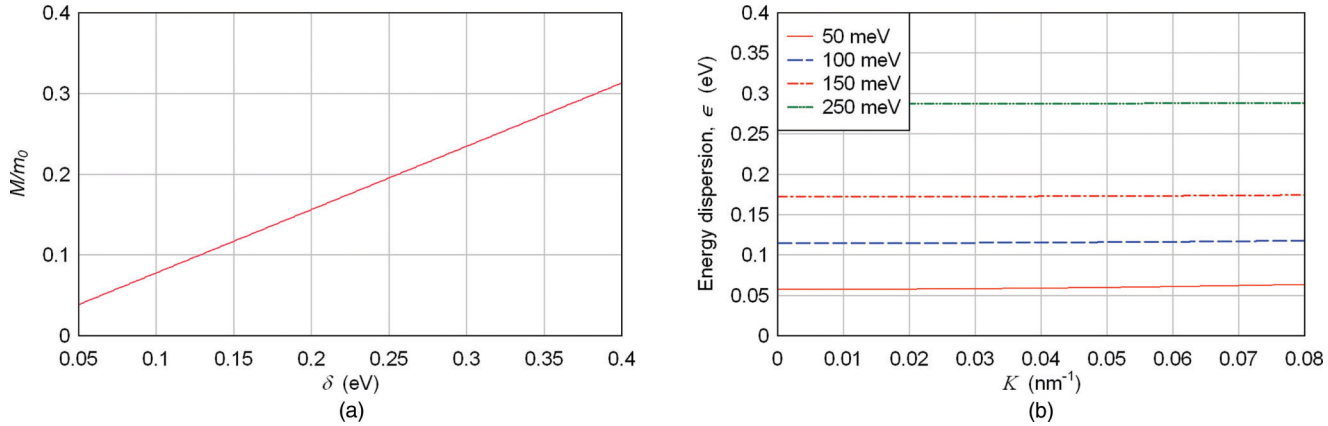

FIG. 3. (Color online) Excitons in the single graphene layer. (a) The effective exciton mass as a function of the energy gap (b) The energy dispersion of excitons in the ground state for the different values of the energy gap.

VI. CONCLUSIONS

Now let us return to the fundamental and practical question related to finding the solution of a problem of two interacting Dirac particles that form the exciton in a gapped graphene layer and in two gapped graphene layers. In the low-energy limit this problem can be solved analytically, and we obtained the energy dispersion and the wave function of the exciton in a gapped graphene layer and in two gapped graphene layers separated by a dielectric. The excitons were considered as a system of two Dirac particles interacting via a Coulomb potential, $V(r)$. In the general case the center-of-mass cannot be separated from the relative motion even though the interaction depends only on the coordinate of the relative motion. The analytical solution for the energy dispersion and the wave function was obtained by introducing the transformation for the separation of the center-of-mass and relative motions for two particles in graphene that allows one to reduce the Dirac-like equation for the spinor to the Schrödinger-like second-order differential equation for the component of the spinor. In the parabolic approximation for the energy dispersion the effective mass of the exciton which is the function of the energy gap in the single graphene layer and function of the energy gaps and interlayer separation in the case of two graphene layers separated by the dielectric is found. First, we can conclude that the exciton effective mass increases in both the case of a single layer of graphene and in the case of two layers of graphene as the gap energy increases. Also the exciton effective mass increases when the interlayer separation increases. Therefore, by tuning the energy gaps in graphene layers and changing the interlayer separation one can get a desirable value for the effective exciton mass. This is very important for the system of many excitons when this system is considered as a dilute gas of excitons that forms Bose-Einstein condensate and undergoes the Kosterlitz-Thouless phase transition to a superfluid phase. By decreasing the mass of the exciton one can increase the Kosterlitz-Thouless transition temperature. Second, for the exciton in a single graphene layer the energy dispersion increases with the increase of the gap energy. However, for the exciton in two graphene layers separated by a dielectric the energy dispersion decreases when the total energy gap increases and it decreases when the interlayer separation increases.

ACKNOWLEDGMENTS

R. Ya. K. is grateful to M. L. Malysh for valuable discussion. K.Z. thanks the Center for Theoretical Physics for hospitality.

[1] L. L. Foldy and S. A. Wouthuysen, Phys. Rev. **78**, 29 (1950).
[2] K. Pachucki, Phys. Rev. A **56**, 297 (1997).
[3] G. P. Lepage, Phys. Rev. A **16**, 863 (1977).
[4] K. Pachucki, Phys. Rev. Lett. **79**, 4120 (1997).
[5] A. Czarnecki, K. Melnikov, and A. Yelkhovsky, Phys. Rev. Lett. **82**, 311 (1999).
[6] J. S. Bell and H. Ruegg, Nucl. Phys. B **98**, 151 (1975).
[7] L. P. Kaptari, A. Yu. Umnikov, S. G. Bondarenko, K. Yu. Kazakov, F. C. Khanna, B. Kampfer, Phys. Rev. C **54**, 986 (1996).
[8] R. Ya. Kezerashvili, Int. J. Mod. Phys. E **6**, 747 (2003).
[9] A. Pineda, Nucl. Phys. Proc. Suppl. **86**, 517 (2000); arXiv:1111.0165v2.
[10] K. S. Novoselov, A. K. Geim, S. V. Morozov, D. Jiang, Y. Zhang, S. V. Dubonos, I. V. Grigorieva, and A. A. Firsov, Science **306**, 666 (2004).
[11] Y. Zhang, J. P. Small, M. E. S. Amori, and P. Kim, Phys. Rev. Lett. **94**, 176803 (2005).
[12] G. W. Semenoff, Phys. Rev. Lett. **53**, 2449 (1984).
[13] D. P. DiVincenzo and E. J. Mele, Phys. Rev. B **29**, 1685 (1984).
[14] A. H. Castro Neto, F. Guinea, N. M. R. Peres, K. S. Novoselov, and A. K. Geim, Rev. Mod. Phys. **81**, 109 (2009).
[15] M. A. H. Vozmediano, M. I. Katsnelson, and F. Guinea, Phys. Rep. **496**, 109 (2010).
[16] A. H. MacDonald, P. M. Platzman, and G. S. Boebinger, Phys. Rev. Lett. **65**, 775 (1990).
[17] P. Littlewood, Science **316**, 989 (2007).

[18] A. A. High, E. E. Novitskaya, L. V. Butov, M. Hanson, and A. C. Gossard, Science **321**, 229 (2008).
[19] I. Carusotto, D. Gerace, H. E. Tureci, S. De Liberato, C. Ciuti, and A. Imamoglu, Phys. Rev. Lett. **103**, 033601 (2009).
[20] R. Johne, I. A. Shelykh, D. D. Solnyshkov, and G. Malpuech, Phys. Rev. B **81**, 125327 (2010).
[21] T. C. H. Liew and V. Savona, Phys. Rev. A **84**, 032301 (2011).
[22] D. W. Snoke, *Solid State Physics: Essential Concepts* (Addison-Wesley, San Francisco, 2009).
[23] A. Amo, T. C. H. Liew, C. Adrados, R. Houdre, E. Giacobino, A. V. Kavokin, and A. Bramati, Nat. Photonics **4**, 361 (2010).
[24] D. W. Snoke, Science **298**, 1368 (2002).
[25] J. M. Kosterlitz and D. J. Thouless, J. Phys. C **6**, 1181 (1973); D. R. Nelson and J. M. Kosterlitz, Phys. Rev. Lett. **39**, 1201 (1977).
[26] O. L. Berman, Yu. E. Lozovik, D. W. Snoke, and R. D. Coalson, Phys. Rev. B **70**, 235310 (2004).
[27] O. L. Berman, R. Ya. Kezerashvili, and K. Ziegler, Phys. Rev. B **85**, 035418 (2012).
[28] O. L. Berman, R. Ya. Kezerashvili, and K. Ziegler, Phys. Rev. B **86**, 235404 (2012).
[29] L. D. Landau and E. M. Lifshitz, *Quantum Mechanics: Non-Relativistic Theory*, 3rd ed. (Elsevier, Oxford, 1977).
[30] R. L. Liboff, *Introductory Quantum Mechanics*, 2nd ed. (Addison-Wesley, Reading, MA, 1992).
[31] D. J. Griffiths, *Introduction to Quantum Mechanics*, 2nd ed. (Prentice-Hall, New York, 2005).
[32] M. I. Katsnelson, Materials Today **10**, 20 (2007).
[33] S. Das Sarma, S. Adam, E. H. Hwang, and E. Rossi, Rev. Mod. Phys. **83**, 407 (2011).
[34] S. Das Sarma, E. H. Hwang, and W.-K. Tse, Phys. Rev. B **75**, 121406(R) (2007).
[35] A. Iyengar, Jianhui Wang, H. A. Fertig, and L. Brey, Phys. Rev. B **75**, 125430 (2007).
[36] J. Sabio, F. Sols, and F. Guinea, Phys. Rev. B **81**, 045428 (2010).
[37] O. L. Berman, R. Ya. Kezerashvili, and Yu. E. Lozovik, Phys. Rev. B **78**, 035135 (2008).
[38] L. Yang, Phys. Rev. B **83**, 085405 (2011).
[39] S. Y. Zhou, G.-H. Gweon, A. V. Fedorov, P. N. First, W. A. de Heer, D.-H. Lee, F. Guinea, A. H. Castro Neto, and A. Lanzara, Nat. Mater. **6**, 770 (2007).
[40] Y. H. Lu, W. Chen, Y. P. Feng, and P. M. He, J. Phys. Chem. B **113**, 2 (2009).
[41] D. Haberer, D. V. Vyalikh, S. Taioli, B. Dora, M. Farjam, J. Fink, D. Marchenko, T. Pichler, K. Ziegler, S. Simonucci, M. S. Dresselhaus, M. Knupfer, B. Büchner, and A. Grüneis, Nano Lett. **10**, 3360 (2010).
[42] D. Alba, H. W Crater, and L. Lusanna, J. Phys. A: Math. Theor. **40**, 9585 (2007).
[43] V. Fock, Z. Phys. **47**, 446 (1928).
[44] C. G. Darwin, Proc. Cambridge Philos. Soc. **27**, 86 (1930).
[45] R. B. Dingle, Proc. R. Soc. London, Ser. A **211**, 500 (1952).
[46] P. A. Maksym and T. Chakraborty, Phys. Rev. Lett. **65**, 108 (1990).
[47] G. B. Arfken, *Mathematical Methods for Physicists*, 3rd ed. (Academic Press, San Diego, 1985).
[48] Yu. E. Lozovik and V. I. Yudson, Sov. Phys. JETP **44**, 38 (1976).
[49] S. Flügge and H. Marschall, *Rechenmethoden der Quantentheorie*, 2nd ed. (Springer-Verlag, Berlin, 1952), problem 24.
[50] B. Zaslow and M. E. Zandler, Am. J. Phys. **35**, 1118 (1967).
[51] X. L. Yang, S. H. Guo, F. T. Chan, K. W. Wong, and W. Y. Ching, Phys. Rev. A **43**, 1186 (1991).